Numerical Modeling and Experimental Verification of Macrosegregation and CET Predictions in Large Steel Roll Ingots

L. Nastac, K. Redkin, C. Hrizo, Sean M. Loney and K. Marsden

Abstract A multi-component Computational Fluid Dynamics (CFD) model developed to study macrosegregation phenomena in 65-tons 2.5 m diameter round-sided steel ingots has been verified through advanced microstructural characterization, chemical analysis and non-destructive testing. Radial and central bars machined out from the full-scale as-cast ingot were compared against the model predictions in terms of columnar-to-equiaxed transition (CET), channel segregation as well as centerline segregation within the central zone of the ingot, which are inherent in the production of industrial scale alloy ingots. The CFD model solves for volume fraction of phases, time-dependent temperature distribution, mass and species transfer to predict segregation patterns in the solidifying ingot. It addresses the influence of various process parameters and mold design aspects on solidification behavior, such as: mold system, pouring rate, superheat, hence, resulted cooling rates, thermal gradients and chemical composition variations. The numerical and experimental results were compared and discussed.

Keywords Roll casting · Steel alloy solidification · Macrosegregation
Columnar-to-Equiaxed-Transition · Computational fluid dynamics (CFD) modeling
and simulation

Introduction

Injecting a dilute steel alloy via a submerged entry nozzle (SEN) into the liquid center of an up-hill teemed net-shaped ingot has been employed on an industrial scale to mitigated undesirable consequences of solute enrichment. Applying an

L. Nastac (✉)
Department of Metallurgical and Materials Engineering, The University of Alabama,
Tuscaloosa, AL 35487, USA
e-mail: lnastac@eng.ua.edu

K. Redkin · C. Hrizo · S. M. Loney · K. Marsden
Whemco, Inc., Pittsburgh, PA, USA

alternative non-SEN (Direct Ladle Pouring) DLP technology to control solidification behavior within the main body section of the net-shaped ingot achieves similar improvement without producing undesirable turbulence. Both the centerline segregation problems and mid-radius channel segregates can be minimized by using these technologies.

A multi-phase, multi-component computational fluid dynamics (CFD) code was used for studying the macrosegregation and columnar-to-equiaxed (CET) formation for a 65-tonne 1.6 m diameter steel roll ingot using the DLP technology. It addresses the influence of various process parameters and mold design aspects such as: mold system, pouring rate and superheat, on the resulted cooling rates, thermal gradients and chemical composition variations. The CFD code solves for the temperature, flow and solute balance in multi-component alloy systems [1].

The ingot segregation model was customized for commercially produced cast steel cast steel back-up roll ingots [2–6]. The CFD multi-phase modeling development effort includes up-hill teeming of the base alloy, SEN or DLP top pouring of the dilute alloy, species transfer during filling, and multi-component segregation during solidification. Customization also includes the development and implementation of initial and boundary conditions, mesh, thermophysical and solidification/segregation properties of the base and diluted steel alloys. A comparison between experimental data and simulation results is provided as well.

Model Description

A comprehensive analysis tool capable to model macro-segregation during ingot casting and solidification of multi-component alloys was developed and implemented into a CFD code. The viscous standard k-ε with standard wall functions, species transport and modified Scheil-based solidification models were used. The Scheil micro-segregation equation was corrected to account for diffusion in the solid phase (e.g., back-diffusion) in a multi-component system based on the microstructure characteristics of the alloy under consideration and the cooling conditions [7–10]. Thus, a framework for studying macro-segregation in various casting processes was developed by solving in a fully coupled mode for the temperature, flow and solute balance in the system. Special flux boundary conditions as a function of time (including the evolution of the air gap at the metal/mold interface) were developed by using experimental temperature data for a 65-tonne 1.6 m diameter steel roll. All thermo-physical properties (including density) and solidification parameters of the steel alloys used in the simulations are functions of temperature.

The CFD model was validated using literature numerical results [11–13]. More literature validation and calibration of the multi-component segregation model was performed using the analytical solution and the experiments in [1–7].

Simulation Conditions

The geometry of the roll is presented in Fig. 1. The process and material parameters for the processed rolls are as follows:

- 10-in (254 mm) wall thickness of the steel body chills (thermally insulated):
- Steel alloy composition of the studied roll (TP is the pouring temperature):
- Up-hill teemed alloy [TP = 2767 F (1793 K)]:
  C = 0.47 wt%, Cr = 4.0 wt%, Mo = 0.7 wt%.
- DLP dilute alloy [TP = 2903 F (1868 K)]:
  C = 0.33 wt%, Cr = 4.0 wt%, Mo = 0.17 wt%.
- 38 min bottom pouring time, 26 min solidification, then 1.5 min top pouring time.
- Cast iron body chills: initial temperature of these chills in the simulated roll is shown in Fig. 1. In the experimental DLP roll, which was cast after the simulation presented in this study was performed, the average temperature of the body chills were: 300 F (422 K), 485 F (525 K), 620 F (600 K), and 730 F (661 K).

Results and Discussion

Figure 2 illustrates the simulation results in terms of liquid fraction, temperature, the liquidus temperature variation (TL) for the DLP roll toward the end of solidification (time = 28 h). Figure 3 presents the predicted C, Cr, and Mo profiles for the DLP roll toward the end of solidification.

Figures 4 and 5 show a comparison of the segregation profiles of predicted and experimental C, Cr and Mo for the DLP case. The simulation results compare favorably with the experimental measurements. The predicted overall dilution and

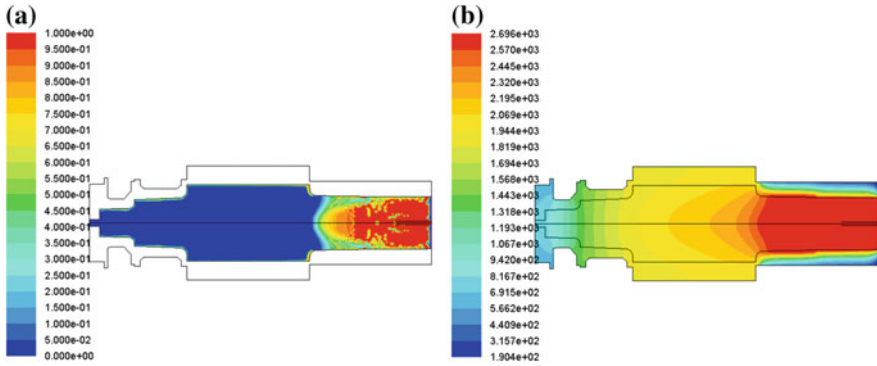**Fig. 1** DLP geometry and the initial temperatures of the steel body-chills

300 F (422 K)   500 F (533 K)   700F (644 K)

1000 F (811 K)

Insulation material   body chill
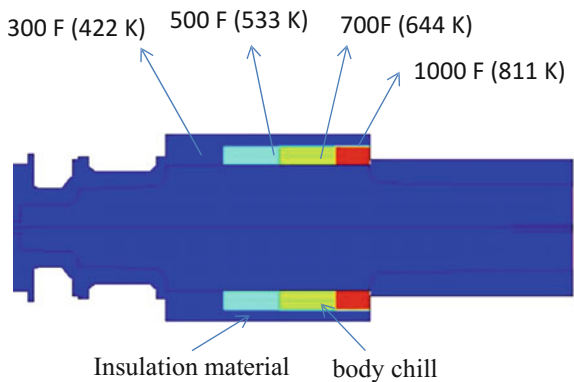
Fig. 2 Liquid fraction (**a**) and temperature (in deg. F) (**b**) distributions at the end of solidification (time = 28 h) in the DLP roll
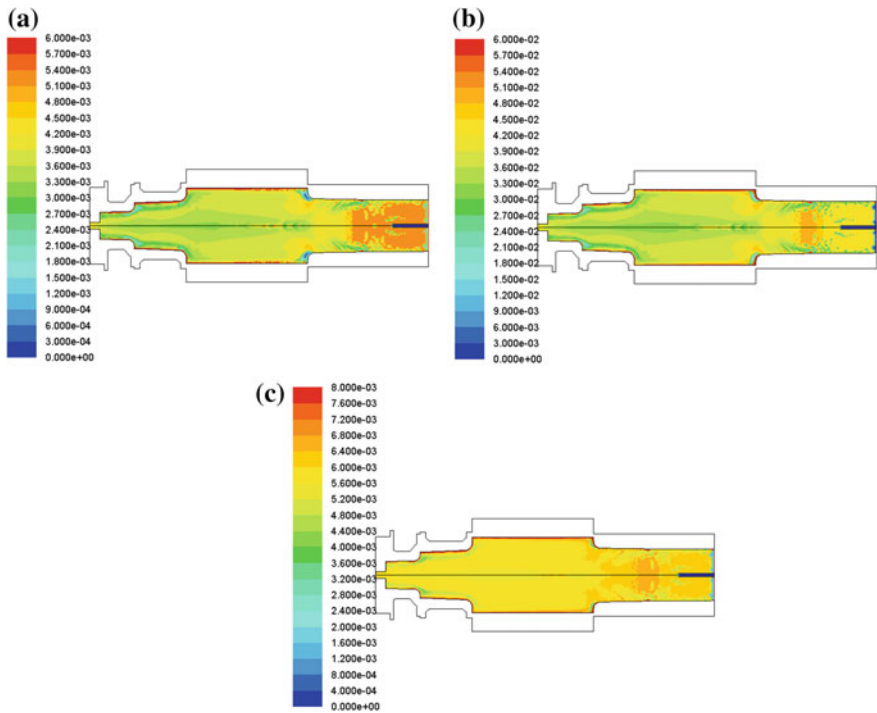

Fig. 3 Distributions of **a** C, **b** Cr, and **c** Mo mass fractions at the end of solidification (time = 28 h) in the DLP roll
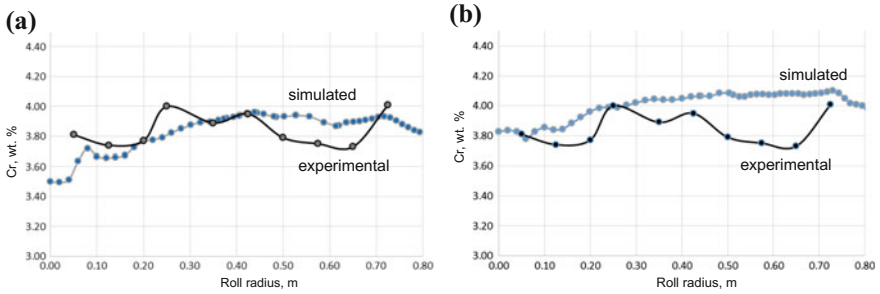
Fig. 4 Comparison of experimental and predicted Cr (in wt%) near the bottom (**a**) and near the top (**b**) of the DLP main body roll

mixing process predicted by simulation compares reasonably well with the experimental measurements except for the top of the roll (Fig. 5). One of the reason is that the temperature of the top body chill (700 F) in the experiment differs from the simulated chill (1000 F). Also, the top pouring process was done with a lip pouring ladle in the experimental roll and with a steel bottom pouring ladle with a 150 mm nozzle in the simulation. Therefore, it is possible that lesser penetration of the dilute alloy that was obtained in the experimental roll was because of these 2 factors. Also, the fusion zone (the distinct area between the shell and core zones) is indeterminate in the DLP process (Fig. 5).
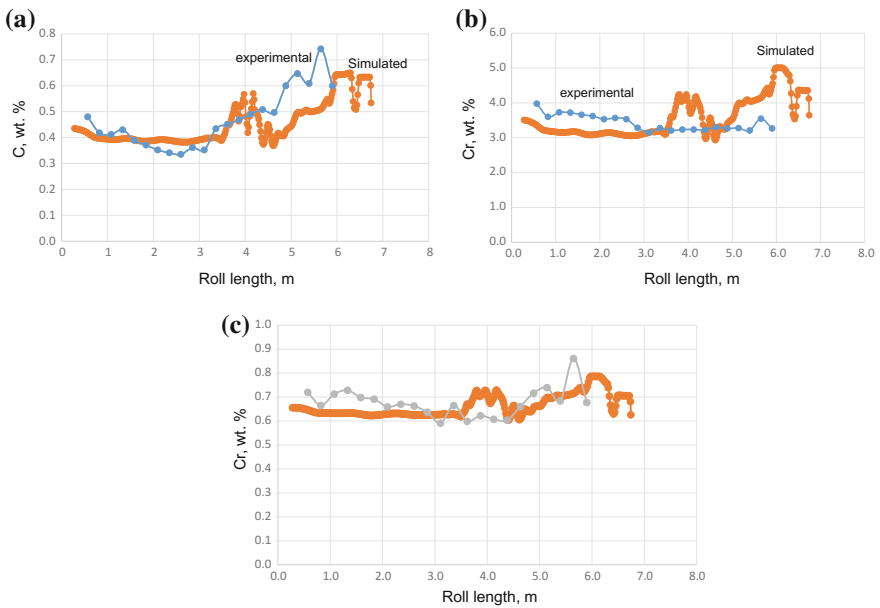

Fig. 5 Comparison of experimental and predicted C, Cr, and Mo (in wt%) centerline segregation along the DLP roll length
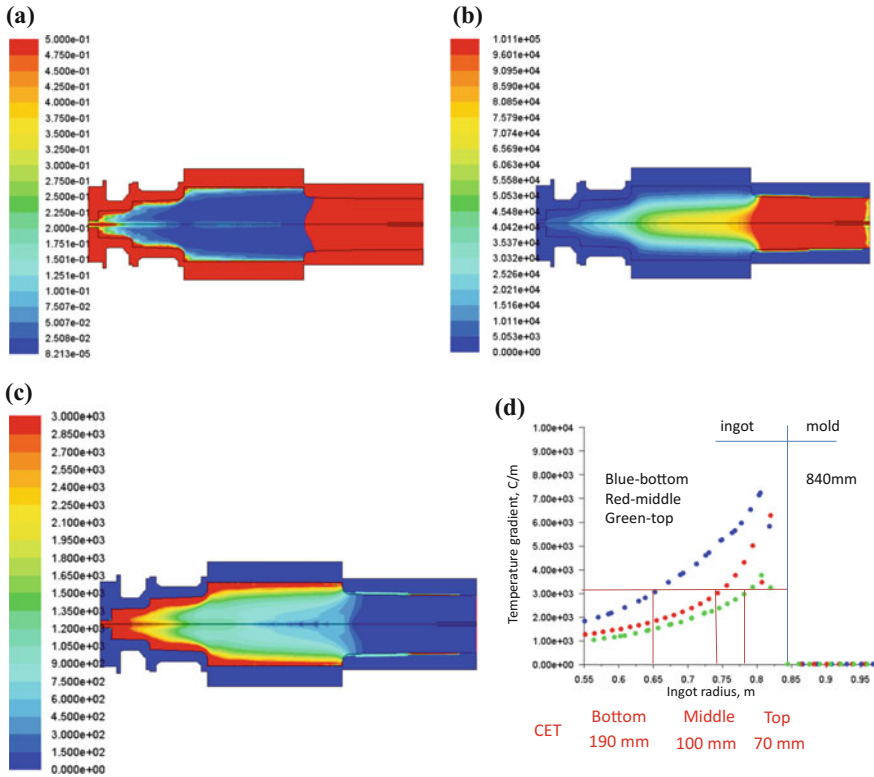
Fig. 6 Distributions of **a** cooling rates (K/s), **b** local solidification times (s), and **c** and **d** temperature gradients (K/m) and (at time = 28 h) in the DLP roll

Figure 6 shows the predicted cooling rates, temperature gradients and local solidification times toward the end of solidification of the DLP roll. The temperature gradients (G, in K/m) (Fig. 6c, d) are computed at the liquidus temperature (*TL*). Columnar-to-equiaxed transition (CET) can be estimated by a critical temperature gradient (G_{cr}) below which equiaxed grains may start to nucleate and grow. Typically, G_{cr} is alloy chemistry dependent and process independent and its value can be estimated via unidirectional solidification experiments. Grain refinement will affect the formation of CET. Normal values of G_{cr} for unrefined dendritic alloys range from 1000 to 5000 K/m. The predicted CET using a $G_{cr} = 3000$ K/m is also shown in Fig. 6c, d.

Figures 7, 8 and 9 illustrate solidification structure characteristics revealed by ultrasonic inspection of the back-up roll produced from the DLP ingot. The CET measurement profile in Fig. 9 matches reasonably the predicted CET in Fig. 6c, d.
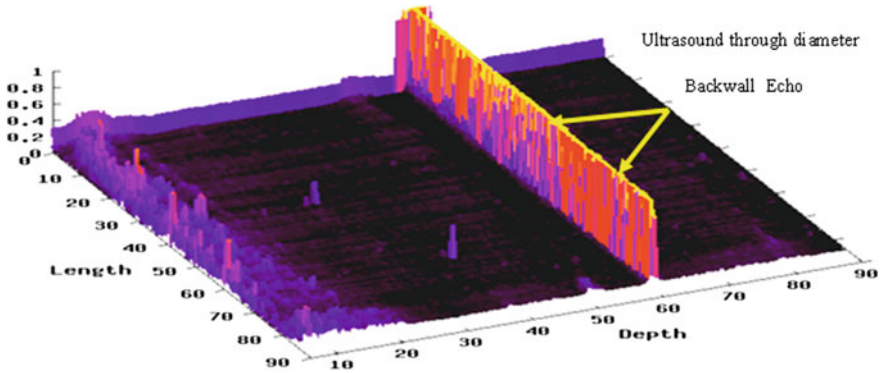
Fig. 7 Conventional ultrasonic inspection through the cross section of the roll
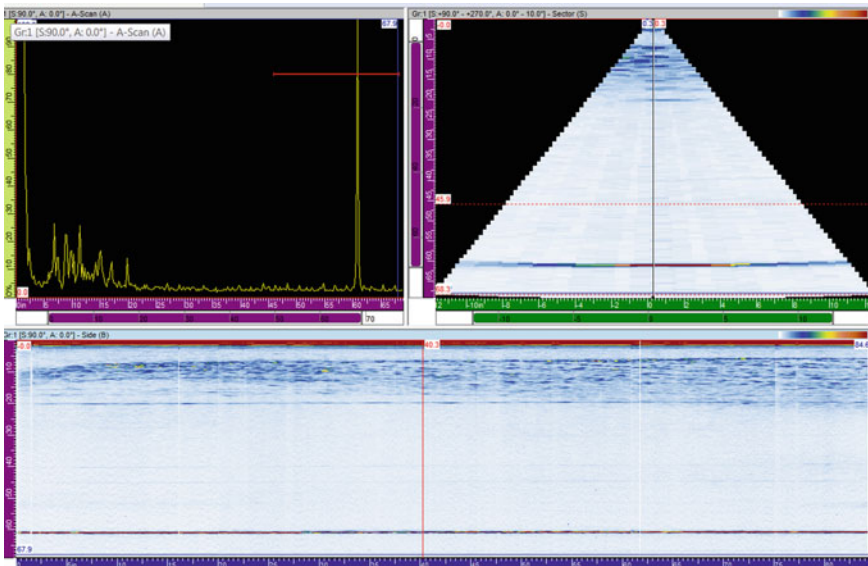

Fig. 8 Phased Array ultrasonic inspection examines the center ingot structure

Figure 10 presents the microstructures at a common radial location near the CET zone on samples removed from the bottom, mid-height and top of the main body section of the net-shaped DLP roll ingot. The microstructures in these samples are equiaxed dendritic with secondary dendrite arm spacing (SDAS) values in the range of 0.5–1.0 mm. By using the local solidification times from Fig. 6b for the location of these samples and the SDAS equation from Ref. [14], a similar range of SDAS values can be predicted based on the current simulation.
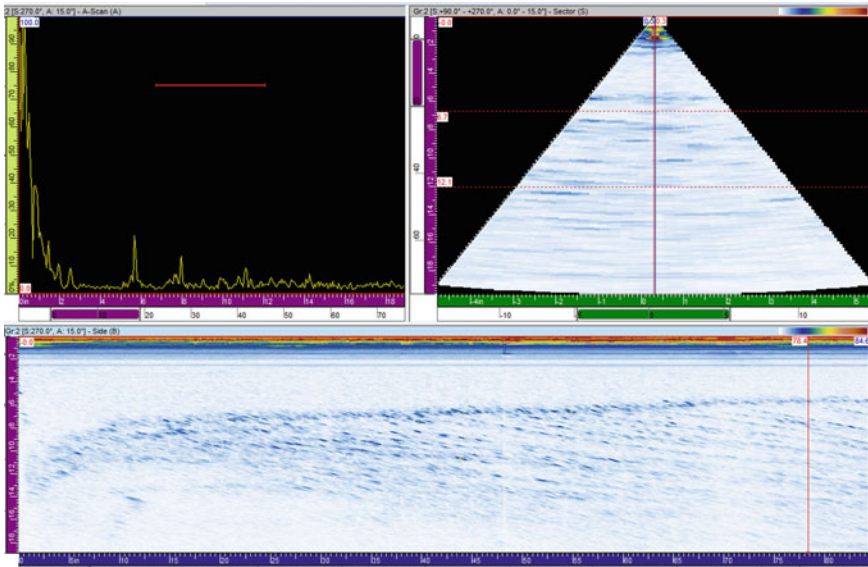
Fig. 9 Phased array ultrasonic inspection of the outer 500 mm zone examines features related to the CET and the channel segregate pattern
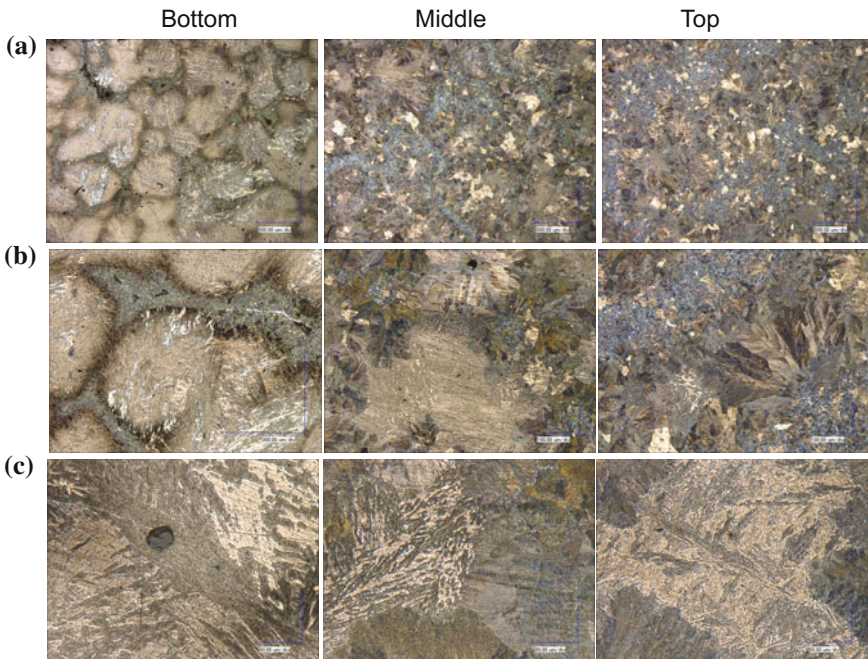

Fig. 10 DLP roll microstructures at ×100 (**a**), at ×300 (**b**) and at ×1000 (**c**)

Conclusions

A numerical modelling approach for predicting macro-segregation in casting was developed and implemented into a CFD code. A validation was performed using experimental measurements for a 65-tonne 1.6 m diameter steel roll that was cast using the DLP technique. The CET predictions match reasonably well the phase array ultrasonic measurements. It was determined that the overall dilution/mixing behavior is comparable for the DLP predictions and experiments except for the top of the roll. Also, the predicted segregation profiles for C, Cr, and Mo compare favorably with the experimental radial and centerline measurements.

References

1. L. Nastac, CFD Modeling of Macro-Segregation during Solidification of Superalloy Castings, The 2nd International Symposium on Cutting Edge of Computer Simulation of Solidification and Casting (CSSC2010), Sapporo, Japan, 2010, *ISIJ*, Vol. 50, No. 12, pp. 1829–1834, 2010.
2. L. Nastac, Computational Fluid Dynamics Modeling of Macro-Segregation and Shrinkage in Large Diameter Steel Roll Castings, *Met Trans B*, 42B, 1231–1243, 2011.
3. Nastac L, Marsden K (2012) Proceedings of ICRF2102, Aachen, Germany, EUROGRESS, 3–7 June 2012, pp 1–10
4. Nastac L, Marsden K (2012) Ninth international conference on CFD in the minerals and process industries CSIRO, Melbourne, Australia, 10–12 Dec 2012, pp 1–6
5. L .Nastac, Numerical Modeling of Macro-Segregation and Shrinkage in Large Diameter Steel Roll Castings: A Mold Study, *International Journal of Cast Metals Research*, Vol. 26, No. 6, pp. 374–82, 2013 (http://doi.org/10.1179/1743133613Y.0000000076).
6. Nastac L, Marsden K (2014) Proceedings of ICRF2014, Milan, 7–9 May 2014, pp 1–7
7. Nastac L (2004) Modeling and simulation of microstructure evolution in solidifying alloys. Springer, New York. ISBN 978-1-4020-7831-6
8. L. Nastac and D. M. Stefanescu, A Model for Solute Redistribution during Solidification of Plate, Columnar or Equiaxed Grains, *Metallurgical Transactions*, Vol. 24A, pp. 2107–2118, 1993.
9. T. Clyne, W. Kurz, Solute redistribution during solidification with rapid solid state diffusion, *Met. Trans A*, 1981, vol. 12A, pp. 965–971.
10. S. Ganguly, S. Chakraborty, A Generalized Formulation of Latent Heat Functions in Enthalpy-Based Mathematical Models for Multicomponent Alloy Solidification Systems, *Met. Trans B*, 2006, vol. 37B, pp. 143–145.
11. P. J. Prescott, F. P. Incropera, Convective transport phenomena and macrosegregation during solidification of a binary metal alloy: I-Numerical predictions, *J. of Heat Transfer*, 1994, vol. 116, pp. 735–749.
12. C. Beckermann, R. Viskanta, Double-diffusive convection during dendritic solidification of a binary mixture, *Physicochemical Hydrodynamics*, 1998, vol. 10, pp. 195–213.
13. M. Rappaz, V. Voller, Modeling of micro-macrosegregation in solidification processes, *Met. Trans A*, 1990, vol. 21A, pp. 749–753.
14. M. El-Bealy and B. G. Thomas, Prediction of Dendrite Arm Spacing for Low Alloy Steel Casting Processes. *Met. Trans B*, 1996, vol. 27B, pp. 689–693.